

# DOMECAIR: AN AIRBORNE CAMPAIGN IN ANTARCTICA SUPPORTING SMOS CALIBRATION

Niels Skou, Steen S. Kristensen, Sten S. Søbjærg, and Jan E. Balling

DTU Space, Technical University of Denmark, Lyngby, Denmark, [ns@space.dtu.dk](mailto:ns@space.dtu.dk)

## ABSTRACT

In search for a stable, well characterized terrestrial calibration target for SMOS, an airborne campaign was carried out in January 2013 over the Dome C area of Antarctica, and the surface was measured by an L-band radiometer. The focus was on homogeneity, and an area of 350 x 350 km around the Concordia station was surveyed using grid, star, and circular flight patterns. Significant and maybe surprising dynamics in brightness temperature is observed. An East-West line through Concordia displays almost 10 K variations, and in specific cases a slope of almost 1 K per km. It is concluded that use of the Dome C area for calibration check of spaceborne radiometers is indeed viable, but with caution – especially when comparing instruments with differing spatial resolutions.

## 1. INTRODUCTION

ESA's SMOS mission is faced with the challenging task of measuring the salinity of the oceans as well as the soil moisture over the continents, based on radiometric measurements of the natural emission from Earth. This is done using a microwave radiometer system operating in the protected radio astronomy band near 1.4 GHz (L-band). Especially the salinity measurements impose severe requirements on the brightness temperature measurement fidelity concerning stability and absolute calibration accuracy. Thus the SMOS instrument features several internal calibration loops, but the important antenna system is outside these loops, and in the end, checks of overall calibration, measuring known external targets, is a necessity throughout the lifetime of SMOS. The problem is that such calibration targets have to be not only stable and well known, but also of very extended size, i.e. hundreds of kilometers, due to the imaging properties of sensors like SMOS.

One of the few feasible terrestrial targets that might live up to all expectations is the area around Dome-C in Antarctica, see Figure 1 displaying Antarctica with the French/Italian Dome-C station, Concordia, indicated. This area will provide SMOS with a hot calibration point. Analysis of existing radiometric measurements (at higher frequencies) from a range of space missions (SMR, SSM-I, AMSR-E) shows good stability and spatial homogeneity.

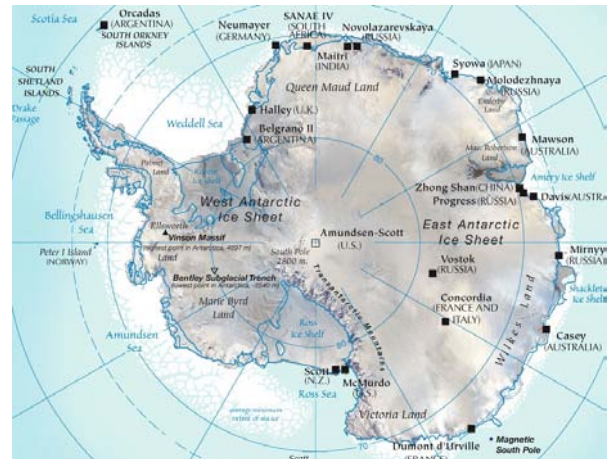


Figure 1. Antarctica with Concordia indicated

An analysis conducted on SMOS data over a two-years period indicates good spatial and temporal stability not only for the area around Dome-C but over a large area of the East Antarctic Plateau. Moreover, the results obtained from ground based radiometric measurements in the DOMEX experiments [1], provides the final confirmation of the good temporal stability. What remains to be investigated in more detail is spatial homogeneity. This can only be done by launching a suitable airborne campaign.

Another natural, extended calibration target is deep space, and indeed SMOS measures this on a regular basis through suitable pitch maneuvers. Deep space, when corrected for galactic radiation, provides a cold calibration point.

Seen from a radiometer designer's point of view this is an ideal situation: the sensor in question regularly measures both a cold and a hot calibration target, meaning that instabilities can be monitored. Since the cold sky can only be measured occasionally (once each fortnight) the Dome-C hot target becomes extremely important as it is measured several times per day! Moreover, and very important: by having both a hot and cold calibration point, problems with possible simultaneous offsets and multiplicative calibration errors can be disentangled.

The temporal stability of the area has already been verified by operating a ground-based L-band radiometer from a tower at Dome-C for a full year,

which demonstrated that especially at V polarization the brightness temperature is very stable showing an annual standard deviation lower than 0.5 K whilst at H polarization it is larger than 1 K because of the effect of snow layering.

Irrespective of this promising result, an open issue to be investigated is the spatial variation of the brightness temperature (TB) at SMOS sub-pixel scale, which is expected to be small around Dome-C. This has, however, never been measured at L-band. Also, a potential azimuth variation (due to for example a predominant wind direction) must be investigated. These issues are deemed important uncertainties and problems with respect to relying on Dome-C as a major SMOS calibration site.

In order to fill this gap ESA launched the DOMEair measuring campaign in the area around Dome-C using a suitable airplane equipped with the EMIRAD L-band radiometer system. This radiometer system was designed for use in a range of airborne campaigns supporting the development of geophysical algorithms for SMOS, as well as being an important instrument in the Cal/Val campaigns. Detailed measurements over a 350 x 350 km area around Concordia were carried out.

## 2. INSTRUMENTATION

### 2.1 EMIRAD-2 L-band Radiometer System

The EMIRAD-2 L-band radiometer system has been developed by Technical University of Denmark, and operated in a range of campaigns, known as the CoSMOS campaigns, in support of SMOS. It is a fully polarimetric (4 Stokes parameters) system with advanced RFI detection features (kurtosis and polarimetry). The system has operated successfully on different aircraft (C-130, Aero Commander, Skyvan) in Denmark, Norway, Finland, Germany, France, Spain, and Australia). The main features of the system are:

- Correlation radiometer with direct sampling
- Fully polarimetric (i.e. 4 Stokes parameters)
- Frequency: 1400.5 – 1426.5 MHz (-3 dB BW) 1392 - 1433 (-60 dB BW)
- Digital radiometer with 139.4 MHz sampling
- Digital I/Q demodulation and correlation for accurate estimation of 3rd and 4th Stokes
- Advanced analog filter for RFI suppression.
- Additional digital filter bank: 4 sub-bands.
- RFI flagging by kurtosis and polarimetry.
- Data integrated to 1 msec recorded on primary storage PC.
- “Fast data” pre-integrated to 14.4  $\mu$ sec. recorded on dedicated PC.
- Sensitivity: 0.1 K for 1 sec. integration time
- Stability: better than 0.1 K over 15 min. before internal calibration.

- Calibration: internal load, noise diode, and Active Cold Load (ACL).
- 2 antennas - one nadir pointing, one side looking at 45 deg. incidence angle
- Antennas are Potter horns with 37.6° & 30.6° half power beam width
- Nadir horn has a 415 m footprint from 600 m flight altitude
- Tilted horn has a 490 m by 640 m footprint, again from 600 m flight altitude.
- Each data package is time stamped using GPS 1PPS signal with 100 ns accuracy.
- Minimum operating altitude: 250 m above terrain @ 140 knots

Further information about EMIRAD-2 is found in [2], and [3].

### 2.2 Airplane

The airplane used for the campaign is a Basler BT-67 owned and operated by the Alfred Wegener Institut (AWI). It is a modified DC-3 with new turboprop engines, and skis for Arctic and Antarctic operation.

Some performance issues are:

- Max speed (wheels only): 225 knots
- Speed for science operations: 165 knots  $\approx$  306 km/h
- Altitude above ground (at Dome-C)  $\approx$  600 m
- Endurance (on skis, at Dome-C): 5 hours
- Max range: 1000 nm

The EMIRAD-2 antennas are installed aft of the wings as shown in Figure 2. One antenna points nadir (not to be seen in the figure), the other is tilted nominally 45° – in this case sideways, using available fuselage apertures.



Figure 2. Basler aircraft with side looking antenna

Previous installations in other aircraft had the tilted antenna pointing aft, and thus ground features were covered with the two incidence angles during the same flight track (very practical for normal, heterogeneous land surfaces). For the quasi-homogeneous ice surface

in question here, it is fully acceptable to divert from this concept and thus not cover exactly the same surface points with the two incidence angles.

To avoid influence from the wing the sideways looking antenna points at  $100^\circ$  relative to aircraft heading, and the incidence angle on ground is  $45^\circ$ .

The radiometer itself is installed very close to the antennas to ensure short antenna cables (low loss), see Figure 3. Also, an inertial navigation unit is mounted close to the antennas in order to measure attitude correctly.



Figure 3. EMIRAD and antennas inside the aircraft

### 3. FLIGHT PATTERNS

In order to evaluate the homogeneity of the area around Dome-C, a raster pattern as shown in Figure 4 was flown (red lines). The area around Concordia is covered by a grid of 11 each 350 km long lines, separated by 35 km. Thus an area of  $350 \times 350$  km is covered. These major grid lines are numbered 1 to 11, line 1 being closest to the South Pole. The area encompasses the Concordia area as well as a triangular area showing especially low and stable brightness temperature [1]. In order to properly cover the area around the Concordia tower based measurements, the lines starts 50 km before Concordia. For this relatively flat and quasi-homogeneous area, the actual altitude is not so important, and radiometer measurements were carried out at constant flight level. The altitude above terrain was roughly 600 m.

In addition to the 11 grid lines, a tie line crossing all other lines (for inter-comparison) is shown.

Normally, during SMOS support campaigns, flights were carried out before dawn in order to totally exclude possible Sun interference. This is not possible for the present campaign where the Sun is always above the horizon. But over the ice cap the situation is benign compared with an ocean situation: we expect

moderate reflected Sun from the surface since this is closer to a blackbody than is the ocean. The DOMEX experiments indeed indicates Sun signals of a certain magnitude, especially at H polarization, such that we have to take them into consideration. In addition we have to take into account direct radiation into the antennas via sidelobes. The EMIRAD-2 antennas are Potter horns, in principle without sidelobes. However, when installed into the metallic airframe this cannot be guaranteed, but very low levels are expected. Thus the direction of the raster pattern lines combined with the time of radiometer data acquisition was planned such that the Sun is never in an angular sector  $100^\circ \pm 45^\circ$  compared to the flight lines (the offset horn looks starboard,  $10^\circ$  aft, and the full main beam is  $\pm 45^\circ$ ). As the Sun moves around by  $360^\circ$  in 24 hours, this means that there is a forbidden time slot at  $11:20 \pm 3$  hours had the lines been east-west. The pattern is rotated by 15 deg. ( $\approx 1$  hour), and thus the forbidden time slot is 7:20 to 13:20. It was therefore planned to take off at 13:30 when covering the lines in the raster pattern. This schedule is also very compatible with the requirements for adequate time for heating and temperature stabilizing the radiometer before use. Irrespective of how well operations try to avoid Sun effects, they will have to be evaluated and possibly compensated, see sub-section about circle flights.

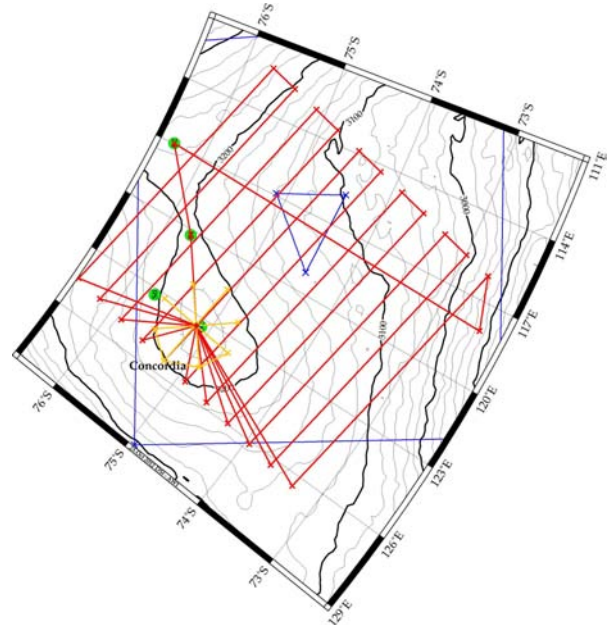


Figure 4. Flight pattern

The area around the tower is covered more intensely by the star pattern also shown in Figure 4 (yellow). The lines are 100 km long. By careful planning it is possible to avoid the Sun affecting the starboard looking horn on all the straight lines.

Several wing wags were carried out for calibration purposes. Those were generally performed when flying

from one line to another, in order not to disturb the data from the proper lines.

Finally, circle flights were carried out to examine a potential azimuthal signature. In order to obtain sufficient radiometric resolution, several circles must be flown and integrated during data processing. Constant roll and pitch angles are important, and thus the aircraft must be left to drift with the wind rather than the pilots try to circle around a fixed point.

In the present experiment, a total of 10 + 10 circles (right-hand / left-hand) were carried out with a bank angle of + and - 10°. This leads to measurements at the following incidence angles: 10°, 35°, and 55°.

In order to evaluate the Sun effect, the circle patterns were carried out twice, many hours apart – early morning and late afternoon. This way it is possible to separate a potential azimuth signature from the ice surface and from the Sun intrusion. The Sun azimuth signature is used to assure that the precautions discussed earlier were adequate – or possibly to correct the raster pattern measurements.

## 4. PREPARATORY EXERCISES

### 4.1 RFI Analysis and Mitigation

The data set has been screened for RFI using methods outlined in [4], that is:

- unrealistic values above 320 K are flagged.
- flagging by kurtosis
- 3rd and 4th Stokes values beyond  $\pm 10$  K are flagged

Global statistics shows that some 3.7% of the data from the nadir horn was flagged, and about 1.4 % from the side looking horn. When subtracting the mean of the cleaned data from the mean of the full, un-cleaned data, the following is noticed: very little difference for the side looking horn. Although RFI is detected, it generally is of quite low intensity.

For the nadir horn, the situation is more diverse: in many data files the difference is again very small, but in a few cases it is significant. As an example, in the first file from the first day (17<sup>th</sup> of January), 3.8 % of the data is flagged, the mean of the full data set is 207.6 K while the mean of the cleaned data set is 205.0 K – i.e. a difference, hence contribution from RFI, of 2.6 K.

In short: there is indeed RFI of significance in Antarctica, but it can be mitigated, and the loss of data is so small that it does not influence final data quality (radiometric sensitivity).

## 4.2 Calibration and Wing Wags

All EMIRAD data was calibrated according to a three step calibration scheme. First, internal calibration is applied, using two of three built-in calibration sources, internal load, ACL, and noise diode. The third calibration point validates the actual calibration, which turns out to be very stable throughout the whole campaign. Second, the microwave cables between the antennas and the receivers are calibrated out using a liquid Nitrogen cooled target, right before or right after each flight, whenever possible. This calibration step shows very consistent results, and estimated parameters for each cable are well in line with factory specifications. For all channels, results are extremely stable throughout the entire campaign. The third calibration step calibrates out the antennas and the Orthomode transducers, using loss and reflection values measured in the laboratory, with a Vector Network Analyzer.

All calibration data is first validated using data from a test flight over the ocean, where wing wags, i.e. large scale variation of the incidence angle, were performed. All data channels show offsets, compared to expected values, but as no in-situ data (wind speed and percentage of ice cover) directly from the test area is available, the absolute level cannot be determined. Wing wags over the ice close to Concordia confirms the presence of offsets between channels, and values, similar to those from the test flight are estimated. Most likely the offsets are caused by small changes in the S-parameters for the antenna system, when installed in the aircraft.

In short, careful calibration has been carried out, but the wing wags show small biases between channels. These biases are estimated, and the channels corrected resulting in the data shown in Figure 5 (nadir and side looking data overlap at 15° – 30°). However, as no external calibration site is available close to the target area, a proper validation of the absolute level cannot be made.

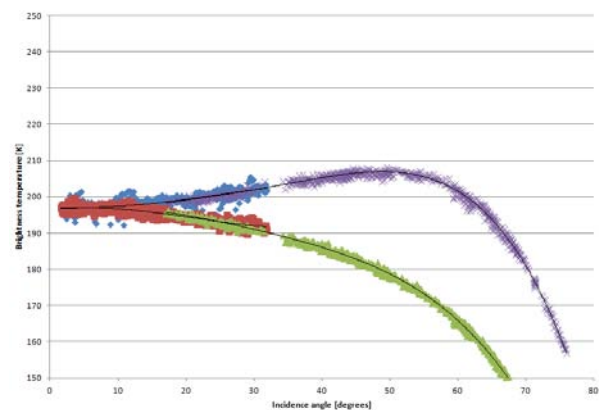


Figure 5. Wing wag data near Concordia

### 4.3 Wag data on DOMEX-3 Data

The wing wag data as discussed in the previous section are well suited for comparison with January 2013 DOMEX-3 data as functions of incidence angle. Figure 6 shows data from [5] with the DOMECAir wing wag data plotted on the same figure (triangles and crosses). The wag data has been adjusted in order to compensate for the different brightness level at Concordia and the wing wag area.

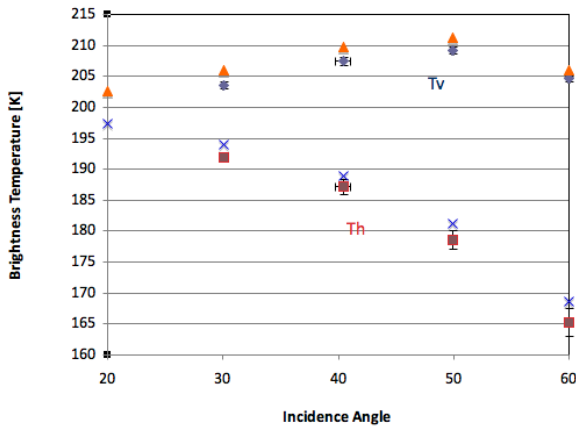


Figure 6. Wing wag data on DOMEX-3 data

It is seen that the 2 sets of curves in general track nicely – but with a 2K bias. However, the comparison is quite satisfactory: we are comparing data from two different instruments each having their individual absolute calibration challenges. It is especially difficult to establish the absolute calibration of the EMIRAD instrument during the campaign, as a sky view is not possible. Also, regularly passing a lake with known temperature and wind conditions (as is routinely done in soil moisture campaigns) is not possible.

### 4.4 Circle Flights

Two circle flights were flown in order to assess azimuth signatures and other azimuth dependent effects such as the Sun and the galactic background radiation. It is evident, that the Sun is far the most important source. It appears clearly in all azimuth signatures, and a worst case of 8 K contribution is found in the 55° AM case, when looking directly to the reflected Sun at H-Pol. Figure 7, where the Sun direction is indicated by the yellow line, illustrates the situation, this time with the 55° PM case. The peak in the H-pol signature is 6 K, slightly lower due to different Sun elevation. 45° from the Sun direction a small contribution is still noted.

The Sun contribution is a strong function of incidence angle, and at the 35° circles it is only 1 K, see Figure 8. The contribution 45° away from the Sun direction is negligible.

Hence the requirement for the flight tracks pointing the side looking antenna more than 45° away from the Sun is justified.

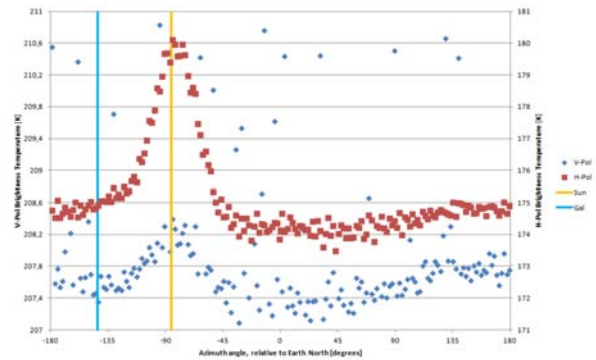


Figure 7. 55° circle signature

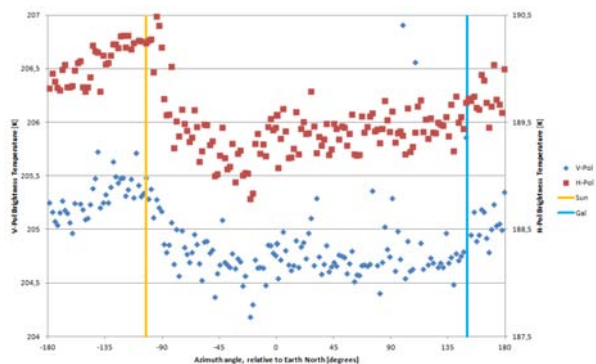


Figure 8. 35° circle signature

The Galactic background theoretically adds a downwelling contribution up to approximately 6 K at worst case, but reflected contributions from the galactic background (blue line in the figures) could not be identified in any case.

Azimuth signatures, not connected to neither the Sun nor the Galaxy, were indicated - especially for the 3rd and 4th Stokes parameters at higher incidence angles. However, the magnitude is so low that it is not significant for our calibration concept.

## 5. TB DATA ON FLIGHT PATTERNS

A good way of giving an overview of the data is to plot TB data on the flight tracks, which as an example is done on Figure 9 for the nadir antenna.

It is seen that the tracks fit well with the plan as shown in Figure 4. Line 1 is at the bottom of the figure while line 11 is at the top. Line 5 passes through Concordia.

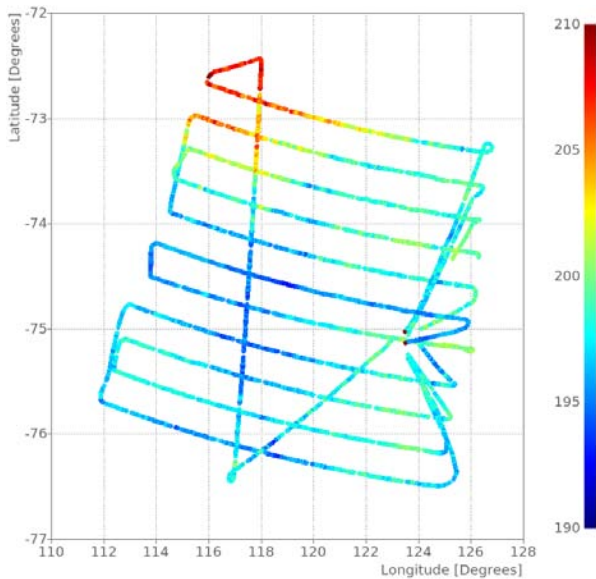


Figure 9. Nadir TB plotted on flight tracks

The dynamic range of brightness temperatures in the plot is approaching 20 K, so it is immediately clear that the Dome C area does not present us with a uniform, homogeneous TB map. Especially the northern part of the plots reveals a significant increase in TB, which of course was already known from SMOS imagery. But also obvious is large smaller scale variation along the lines.

## 6. 2D IMAGERY

The data set already discussed in the previous chapter has been smoothed in order to provide 2D imagery of the area, see Figure 10 as an example for the side looking antenna.

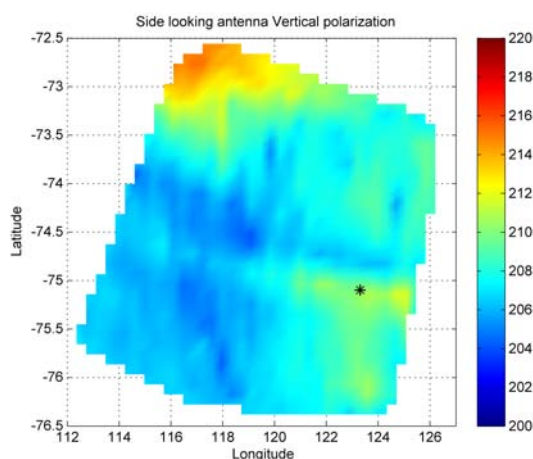


Figure 10. Side looking TBV data

The relatively large dynamic TB range as already noted in Section 5 is again easily seen. Especially the

northern part of the image reveals a significant increase in TB. But also the area around Concordia (indicated by the \*) actually is situated on a TB hilltop overlooking lowlands in most directions. This of course presents special challenges when comparing DOMEX data with DOMECAir data.

The low TB area (around lat. 74 – 75.5 & lon. 116 – 119) is clearly revealed.

## 7. PROFILES

The data from the 11 grid lines and the tie line has been processed as profiles, see Figure 11, which shows line 5 side looking data as an example.

We generally observe a significant dynamic range even without taking the warm northern area into consideration. For example line 5, side looking V pol, displays values from 205 K to 213 K. Line 5, side looking H pol, shows around 60 km a variation of 4.5 K over 6.5 km, i.e. a slope of almost 1 K / km!

We note from the profiles the area with consistent, low TB values – but it is in fact not very homogeneous, especially in the east-west direction (see line 5, Figure 11, 60 – 130 km), while it is somewhat better in the north-south direction (tie line, not shown here). This observation is consistent with the texture as seen in the 2D imagery in Figure 10.

By zooming in on profiles like the one in Figure 11, details can be studied. Noting that the antenna footprint is around 500 m and the radiometric sensitivity is 0.1 K i.e. a 0.3 K p-p appearance in the plots, we see a mixture of  $\Delta T$  and small resolved wiggles in the plots. Also, we see somewhat larger, certainly resolved wiggles / waves. In the full range profiles, as shown in Figure 11, is clearly seen larger variations as well as tendencies from beginning to end of the profiles.

In conclusion: significant brightness temperature variations are observed over different scales ranging from a few km to 350 km.

In order to assess the influence of the inhomogeneities when observing the area with SMOS and Aquarius eyes, the profiles of the side looking antenna have been convolved with 43 km and 100 km 3dB beamwidth antenna pattern replicas (Gaussian shape). When convoluting the antenna patterns with the survey lines the outermost 100 km at both ends of each survey line become invalid in the Aquarius case due to the width of the Aquarius antenna pattern replica. Hence, only the parts within 100 km of the ends of each survey line is used. An example using grid line 2 is shown in Figure 12.

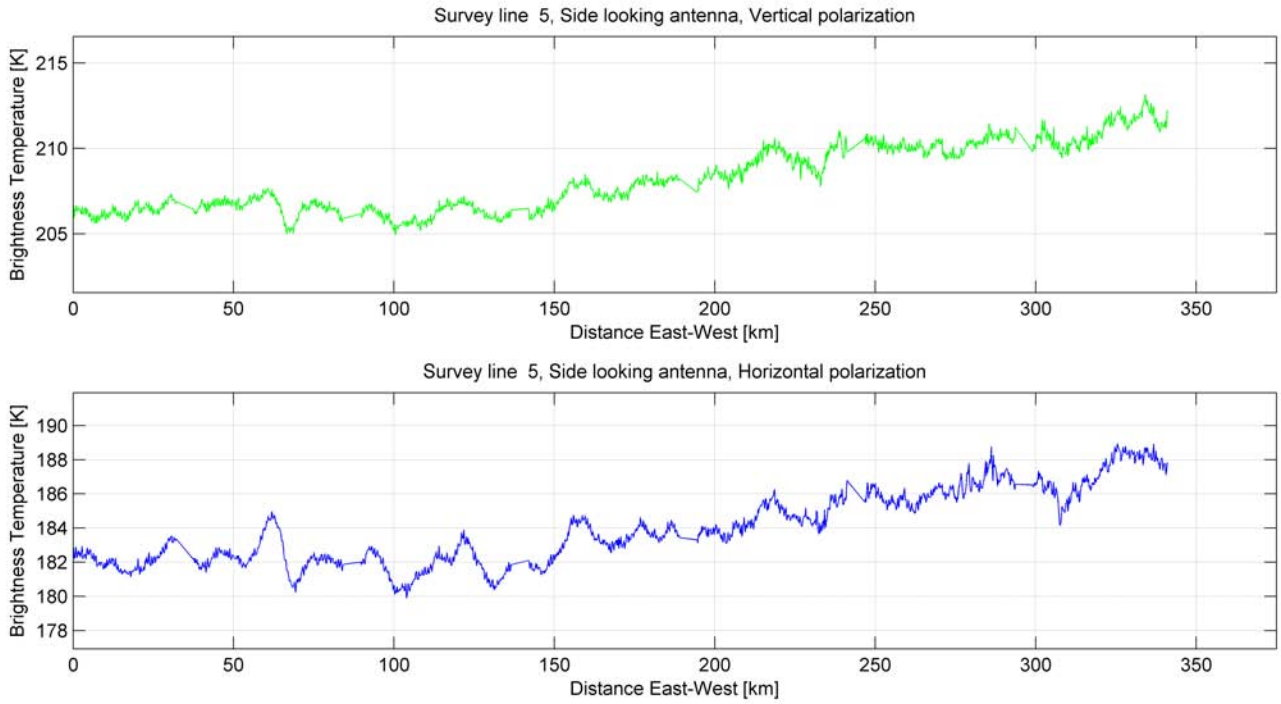


Figure 11. Grid line 5, side looking antenna

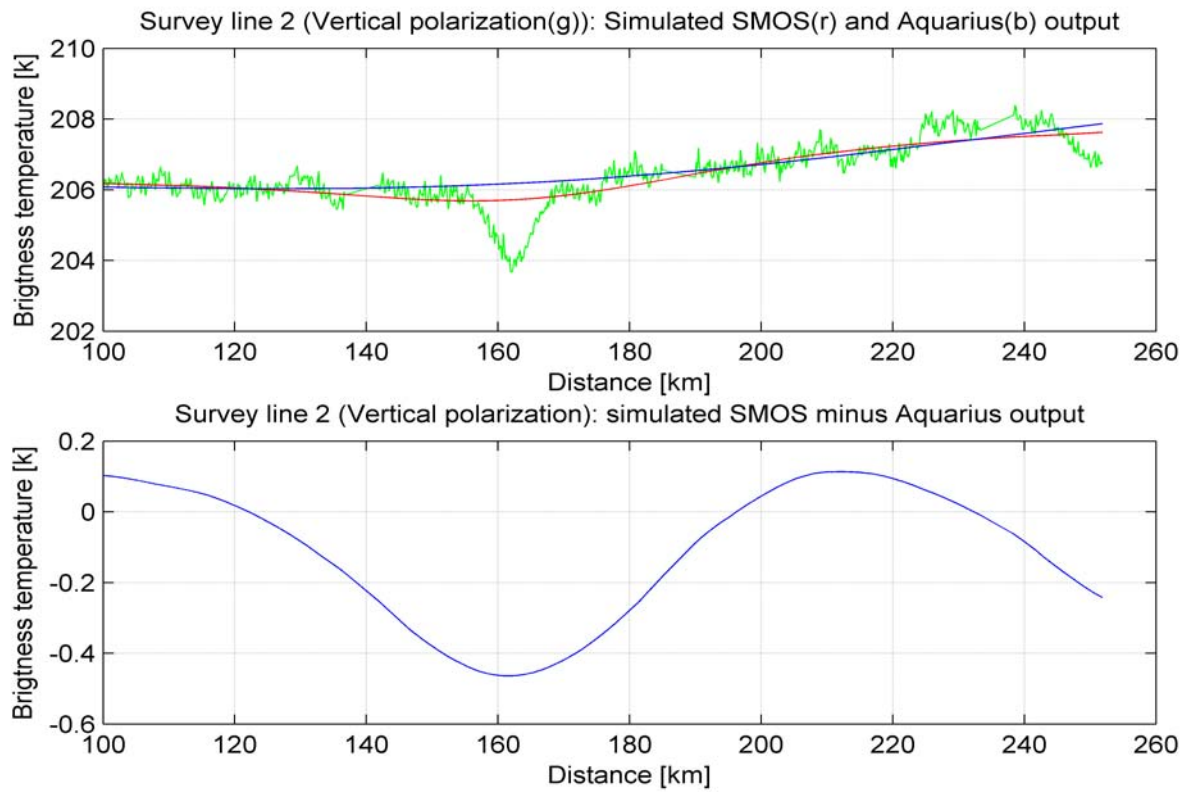


Figure 12. Central part of line 5, integrated to SMOS and Aquarius

In the simulated SMOS and Aquarius outputs it is clearly seen how wiggles and waves are integrated out, leaving only large variations and tendencies. But it is also seen how there are significant differences between SMOS and Aquarius – in the present example by up to 0.4 K, which is a typical max value. The worst difference noted is 0.8 K.

Statistical analysis shows that the mean value of the difference SMOS – Aquarius is negative. This is very important because it shows that there will be a systematic difference between SMOS and Aquarius measurements at this site. The reason for this systematic difference is that this site to some extent is a local minimum, and Aquarius will measure a higher brightness temperature at local minima due to its wider antenna 3dB width.

## 8. DISCUSSION AND CONCLUSIONS

A potential calibration site for SMOS, situated in the Dome C area of Antarctica, has been investigated using radiometric measurements from an airborne campaign. The 350 x 350 km area turns out to be less spatially homogeneous at L-band frequencies than previously assumed. The range of brightness temperatures within the area approaches 20 K, and disregarding the warm northern corner, where elevation drops, still 10 K variations across the area are noted. The dynamics are also illustrated by an example where the brightness temperature drops by 4.5 K over 6.5 km, i.e. a slope of almost 1 K / km. In short: significant brightness temperature variations are observed over different scales ranging from a few km to beyond 300 km.

The relatively large footprints of SMOS ( $\approx 40$  km) and Aquarius ( $\approx 100$  km) will smooth out rapid variations, but longer variations and tendencies result in differences of typically up to 0.5 K between the 2 instruments. Furthermore, the difference (SMOS – Aquarius) is biased negative due to the fact that the area in question is a local minimum concerning brightness temperature.

As part of the campaign, circle flights were carried out in search for possible azimuth signatures. Apart from the obvious signal from the Sun no significant geophysical signature could be identified. Also, during the campaign, wing wags were carried out in support of calibration activities, and the brightness temperature variation with incidence angle compares well with similar data from the tower based DOMEX-3 measurements.

Finally it is noted that there is indeed RFI in Antarctica, and globally a few percent of data had to be flagged.

In conclusion, the authors recommend that the Dome C area can be considered as a viable calibration site, but care must be exercised when planning which footprint positions to evaluate for calibration reference, and for sensor inter-comparison.

## ACKNOWLEDGMENTS

The authors would like to thank T. Casal and M. Davidson, ESA, for supporting the campaign in many ways including planning and discussion of results. Also many thanks go to D. Steinhage, AWI for his contribution to planning and carrying out the campaign.

## REFERENCES

1. Macelloni, G., Brogioni M., Pettinato S., Montomoli F., Monti F., and Casal T. (2013). L-band Characterization of Dome-C Region using Ground and Satellite Data. *IGARSS'13*, pp. 3427-3440.
2. Skou, N., Søbjærg, S. S., Balling, J., Kristensen, S. S. (2006). A Second Generation L-band Digital Radiometer for Sea Salinity Campaigns. *IGARSS'06*, 4p.
3. Søbjærg, S. S., Kristensen, S. S., Balling, J., Skou, N. (2013). The Airborne EMIRAD L-band Radiometer System. *IGARSS'13*, pp. 1900-1903.
4. Balling, J. E., Kristensen, S. S., Søbjærg, S. S., and Skou, N. (2011). Surveys and Analysis of RFI in Preparation for SMOS: Results from Airborne Campaigns and First Impressions from Satellite Data. *IEEE Trans. on Geoscience and Remote Sensing*, Vol. 49, No. 12, pp 4821-4831.
5. Macelloni, G., personal communication.